ADVANCED SUSTAINABLE SYSTEMS
www.advsustainsys.com

The Rapid Mechanochemical Synthesis of Microporous Covalent Triazine Networks: Elucidating the Role of Chlorinated Linkers by a Solvent-Free Approach

*Annika Krusenbaum, Fabien Joel Leon Kraus, Stefanie Hutsch, Sven Grätz, Mark Valentin Höfler, Torsten Gutmann, and Lars Borchardt**

The mechanochemical synthesis of porous covalent triazine networks (CTNs), exhibiting theoretically ideal C/N ratios and high specific surface areas, is presented. Employing this solvent-free approach allows to minimize the ecological impact of the synthesis by bypassing hazardous wastes, while simultaneously observing the reactions between the individual starting materials separately for the first time. Especially the role of dichloromethane needs to be reconsidered, functioning as a linker between the nitrogen-containing node cyanuric chloride and the aromatic monomer 1,3,5-triphenylbenzene, as proven by X-ray photoelectron spectroscopy and $^{1}H \rightarrow {}^{13}C$ Cross-Polarization magic-angle-spinning nuclear magnetic resonance spectroscopy. This results in a drastic enhancement of the reaction rate, reducing the synthesis time down to 1 minute. Additionally, this linkage over a C1 bridge enables the incorporation of nitrogen into already synthesized polymers by post polymerization functionalization. The variation of the synthesis building blocks, namely the linker, node, and monomer, results in a variety of nitrogen-containing polymers with specific surface areas of up to 1500 $m^2 g^{-1}$. Therefore, the presented approach is capable to target the synthesis of various CTNs with a minimal use of chlorinated linker, rendering the concept as a sustainable alternative to the classical solution-based synthesis.

1. Introduction

Porous polymers recently received increasing attention, as they can be utilized in a wide range of diverse applications, such as in catalysis, in molecular separations, or in gas and energy storage.[1–12] In this regard, the scientific focus lately shifted to porous organic polymers (POPs), as their template-free modular design principle enables the generation of structurally flexible and lightweight materials, exhibiting heteroatom functionalities as part of the pore walls.[13–15] An important subgroup of this material class comprises of triazine-based POPs, possessing significant chemical and thermal stabilities, as well as high amounts of nitrogen, resulting in a certain hydrophilicity of the polymer.[16,17] Additionally, the introduction of these nitrogen functionalities enables the coordination of metal particles for application in catalysis, or can be used to enhance gas uptake capacities in gas storage devices due to an electrostatic interaction between the nitrogen-containing moiety and the gas molecules.[18–29]

Initially, the generation of porous triazine-containing polymers was achieved by ionothermal trimerization of aromatic nitriles in molten $ZnCl_2$, requiring harsh reaction conditions of 400–600 °C.[25,30–32] To circumvent the high melting point of $ZnCl_2$, and thereby an accompanied undesired carbonization of the polymer, the reaction can be carried out either in an eutectic salt mixture or in a microwave, still requiring a reaction temperature of 200 °C or exhibiting a challenging reaction control, respectively.[33,34] Alternatively, the trimerization can be achieved by catalysis with a strong Brønsted acid, such as trifluoromethanesulfonic acid.[24,26] However, one distinct disadvantage of all trimerization approaches is the requirement of aromatic nitriles, drastically limiting the substrate scope. To obviate this and to achieve a cost-effective and versatile synthesis protocol, a Friedel–Crafts reaction can be applied to initiate the copolymerization of two reactants, one of which is bearing the triazine node.[27,35] Therefore, a Lewis acid is utilized to knit the aromatic monomer and the nitrogen-containing node under reflux in a halogenated solvent for 16 h or more.[36,37]

To circumvent the requirement of toxic solvents and the accompanied generation of high amounts of hazardous waste, a solvent-free mechanochemical synthesis approach can be applied.[38–41] Therein, the reaction between the starting

A. Krusenbaum, F. J. L. Kraus, S. Hutsch, S. Grätz, L. Borchardt
Inorganic Chemistry I
Ruhr-Universität Bochum
Universitätsstraße 150, 44780 Bochum, Germany
E-mail: lars.borchardt@ruhr-uni-bochum.de
M. V. Höfler, T. Gutmann
Technical University Darmstadt
Institute for Inorganic and Physical Chemistry
Alarich-Weiss Straße 4, 64287 Darmstadt, Germany

DOI: 10.1002/adsu.202200477

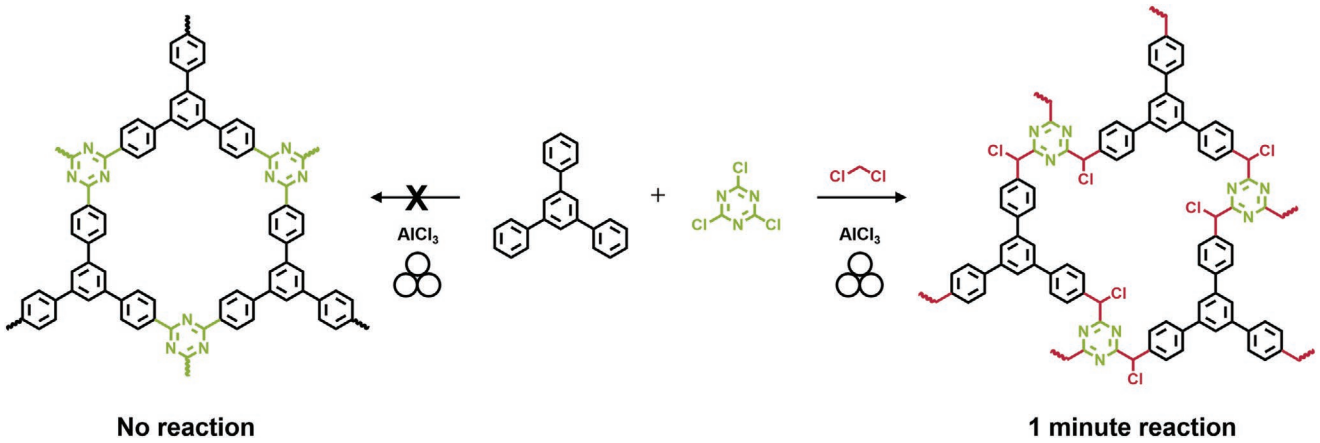

Figure 1. Schematic overview over the mechanochemical synthesis of porous covalent triazine networks (CTNs). The solvent-free approach enabled to directly observe the reaction between the monomer 1,3,5-triphenylbenzene and the node cyanuric chloride, not leading to any product (top, left side). Therefore, the role of the linker dichloromethanewas highlighted, resulting in the formation of a highly porous and nitrogen-containing polymer after a synthesis time of 1 min (top, right side). This concept was applied to a variety of nodes, monomers, and linkers, enabling the targeted synthesis of various CTNs.

materials is induced by mechanical force, circumventing a low degree of polymerization due to an instant precipitation of the polymers, the requirement of additional synthesis steps for the introduction of solubilizing groups, and the need for expensive catalysts. Furthermore, the constant mixing of the reactants results in the permanent creation of reactive surface, reducing the synthesis time from several hours to minutes, which renders this concept economically and ecologically favorable.[42–47]

Initially, the mechanochemical Friedel–Crafts reaction toward nitrogen-containing POPs was achieved by the use of harsh reaction conditions, as for example by the utilization of high-density milling materials, which can lead to the abrasion of the milling material.[48] Additionally, the stress generated by the high energy input results in a heating of the system to >60 °C and in a partial degradation of the newly synthesized polymers.

In order to circumvent the accompanied problems, such as low yields and low specific surface areas for the utilization of certain aromatic monomers, we herein present a novel mechanochemical synthesis approach for the rapid and sustainable generation of highly porous covalent triazine networks (CTNs). Due to this approach, it was not only possible to obtain nitrogen-rich polymers in yields of up to >99%, while drastically reducing the E-factor in comparison to the solution-based reaction; the solvent-free synthesis furthermore enabled to elucidate the polymer formation in more detail. Thereby, it was feasible to observe the reaction between the individual starting materials separately for the first time (**Figure 1**), leading to a revaluation of the role of the halogenated liquid and to a newly proposed reaction mechanism. The halogenated liquid was found to serve as a C1 linker between the monomer and the node (Figure 1 right side), although it was formerly considered to act only as a solvent.[22,27,35,36,37,49,50,51,52,53,54] This observation not only prompted the functionalization of purely carbon and hydrogen-containing polymers by post polymerization, rather it even enabled the modification of various building blocks to receive porous nitrogen-containing polymers with specific surface areas of up to 1500 $m^2\ g^{-1}$. Since the versatile synthesis protocol led to an enhancement of reaction rate, a highly porous and nitrogen-containing polymer could be obtained within 1 min of reaction time. Hence, the presented approach proved to be a sustainable alternative for the rapid generation of CTNs at room temperature.

2. Results and Discussion

2.1. Analysis of CTN

The mechanochemical synthesis of porous CTN was achieved by the Friedel–Crafts polymerization of an aromatic monomer and a nitrogen-containing node under mild conditions. Please note the difference between CTNs and CTFs—covalent triazine frameworks. While the former describes a triazine-containing network, the latter explicitly refers to a crystalline framework (see Figure S1, Supporting Information).

In a typical synthesis approach the monomer 1,3,5-triphenylbenzene (TPB) (0.50 g, 1.63 mmol, 1 equiv.) and the node cyanuric chloride (CyCl) (1.81 g, 9.79 mmol, 6 equiv.) were knitted by the addition of 0.63 mL (9.79 mmol, 6 equiv.) dichloromethane (DCM) under Lewis acid catalysis. Since the utilization of other catalysts did not facilitate the formation of a porous and nitrogen-containing polymer, aluminum(III) chloride ($AlCl_3$) (5.22 g, 39.16 mmol, 24 equiv.) was applied to function as both Lewis acid and as bulk material. After the sophisticated milling at 30 Hz for 1 h in a MM500 mixer mill, the crude product was shortly rinsed with water and acetone and was dried at 80 °C over night. The resulting brown polymer **CTN-1** was obtained in 95% yield and will serve as a reference system herein.

CTN-1 is featuring a specific surface area (SSA_{BET}) of 1136 $m^2\ g^{-1}$ and an IUPAC type I isotherm with a steep volume uptake in the micropore region (see **Figure 2**I). The isotherm exhibits a pronounced swelling behavior, which indicates the flexible nature of the polymer. The polymer is highly microporous with a main pore width of 0.67 nm, which is in a comparable range to pore sizes observed for similar polymers synthesized

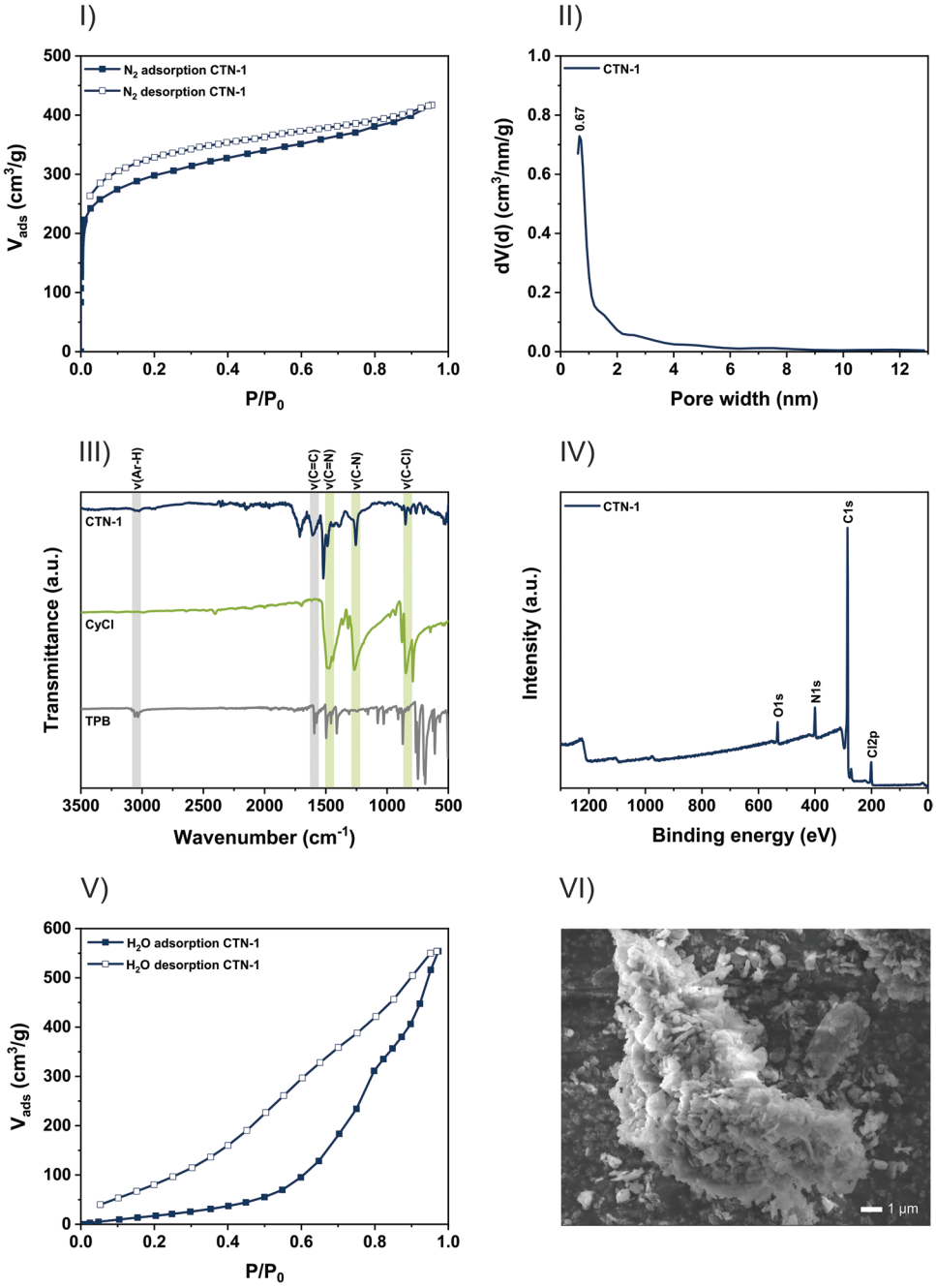

Figure 2. Analysis of the covalent triazine network **CTN-1**. I) N_2 physisorption isotherm of **CTN-1** measured at 77 K. II) Pore size distribution of **CTN-1** for pore widths between 0 and 13 nm by DFT calculation applying the calculation model N2 at 77 K on carbon (slit pore, QSDFT equilibrium model). III) FT-IR spectra of **CTN-1** (in blue), of CyCl (in green), and of TPB (in grey) with vibrations assigned to **CTN-1** in the color of their origin (either from TPB (grey bars), or from CyCl (green bars)). IV) XPS survey spectrum of **CTN-1** showing oxygen (O 1s), nitrogen (N 1s), carbon (C 1s), and chlorine (Cl 2p) inside the polymer. V) Water sorption isotherm of **CTN-1** measured at 298 K. VI) SEM image of **CTN-1** with a scale of 1 µm.

by solution-based protocols (ranging between 0.73 and 1.18 nm) (see Figure 2II).[27]

To verify the incorporation of the nitrogen-containing node into the polymer, FT-IR analysis was carried out, showing very distinct vibrations ascribed to a well-defined material (see Figure 2III). The vibrations in the spectrum of **CTN-1** can be attributed to certain characteristics of the monomer or the node, respectively. For example, the Ar—H stretching vibration at 3040 cm^{-1} is visible for **CTN-1** (Figure 2III in blue) as well as for the aromatic monomer TPB (Figure 2III in grey). In addition to this, both spectra feature a C=C stretching vibration at 1600 cm^{-1}. Likewise, the characteristic bands for CyCl (Figure 2III in green), which are a C=N stretching vibration at 1490 cm^{-1} and a C—N stretching vibration at 1270 cm^{-1},

are also present in the spectrum of **CTN-1**. Additionally, a C—Cl stretching vibration is visible at 850 cm^{-1}, assigned to remaining chlorine atoms attached to the polymer. Indeed, X-ray photoelectron spectroscopy (XPS) reveals a contamination of 3.4 at% Cl, as well as of 3.4 at% O (see Figure 2IV and Table S2, Supporting Information), which is matching perfectly to the theoretical value of 3.2 at% for the formation of CHCl moieties in the polymer (see subsequent chapter). The peak with the highest intensity in the XPS survey spectrum is ascribed to carbon, which is present with 85.6 at% in the polymer. The C 1s spectrum of **CTN-1** (see Figure S2, Supporting Information) clearly indicates the presence of three different carbon species, attributed to sp^2 hybridized carbon in the aromatic rings (284.0 eV), to sp^3 hybridized carbon (284.6 eV) and to C=N binding in the triazine rings (285.0 eV). The nitrogen itself is present with 7.6 at% in **CTN-1** and the N1s spectrum comprises of only one peak, showing the nitrogen atoms of the triazine moiety (399.7 eV) (see Figure S3, Supporting Information).

As the incorporation of the triazine unit into **CTN-1** results in a higher hydrophilicity of the polymer, water sorption was carried out (see Figure 2V). The outcome was compared to the homocoupling-polymer **FC-DCM-1** containing no nitrogen (Figure S4, Supporting Information), but featuring a similar SSA_{BET} of 1121 $m^2\ g^{-1}$. Indeed, **CTN-1** was found to be more hydrophilic than the highly hydrophobic **FC-DCM-1**, as it exhibits an earlier onset of water uptake at around $P/P_0 = 0.2$ in comparison to $P/P_0 = 0.5$ for **FC-DCM-1**. Additionally, although both polymers feature similar specific surface areas, the total pore volume for water uptake of **CTN-1** (0.45 $cm^3\ g^{-1}$) is much higher than of **FC-DCM-1** (0.19 $cm^3\ g^{-1}$) at $P/P_0 = 0.97$. Furthermore, the high discrepancy between adsorption and desorption of water molecules, achieved by adhesion of the adsorbate on the surface of the adsorbent, hints toward a higher hydrophilicity of **CTF-1** due to incorporated nitrogen.

Following these investigations, **CTN-1** is proved to be comprising of the starting materials. The homogeneous nature and the rough surface of the polymer are furthermore visible in the SEM image (see Figure 2VI).

2.2. Reaction Mechanism Elucidation

The synthesis of **CTN-1** was carried out with 6 equiv. of the node CyCl to achieve the formation of a highly porous nitrogen-containing polymer. Interestingly, the excess of node did not result in a higher yield compared to **CTN-2**–**CTN-6**, synthesized with lower amounts of node equivalents (see Table S1 and Figure S5, Supporting Information). In each of these cases, the yield was close to the theoretical yield, calculated for the incorporation of only 1 equiv. of the node, regardless the number of equivalents utilized during the syntheses (Figure S5, Supporting Information). This was additionally confirmed by investigating the C/N ratios of the respective polymers. Whereas the theoretical C/N ratio for the incorporation of 1 equiv. of node is 11.05, higher amounts of nitrogen-containing node would lower the C/N ratio to up to 2.67 for the incorporation of all 6 equiv. (Figure S6, Supporting Information). Nevertheless, **CTN-1** exhibits a C/N ratio of 11.26, which proves that only one equivalent of node is built into the polymer. Although an excess of CyCl does not lead to a higher amount of nitrogen in the polymer, it did increase the specific surface area from 658 $m^2\ g^{-1}$ (1 equiv. node [**CTN-2**]) to 1136 $m^2\ g^{-1}$ (6 equiv. of node [**CTN-1**]) (Figure S6, Supporting Information). Hence, the remaining equivalents of the node that are not incorporated into the polymer likely serve as porogen for pore formation during the polymerization and are removed by the workup (Figure S7, Supporting Information).

In addition to the special role of the node, DCM is of tremendous importance for the polymerization. In the classical solution-based chemistry, the syntheses of porous triazine-containing polymers are mainly attributed to a direct reaction between the aromatic monomer and the nitrogen-containing node under Lewis acid catalysis and with DCM serving as a solvent (**Figure 3**III, Top).[27,35,36] Therein, $AlCl_3$ is proposedly attacked by the chlorine atom of the CyCl, resulting in a positive charge at the carbon atom of the node. This can be attacked by the high electron density of the monomer, resulting in a new C—C bond formation under the release of HCl and by rearomatization of the monomer. However, the attack of the $AlCl_3$ from the halogen alkene is highly unlikely, as the corresponding cation is energetically unavailable.[55] Furthermore, the halogenated liquid DCM is theoretically capable to participate in the reaction, although it is generally considered to act only as the solvent and not as a co-reactant.

A solvent-free mechanochemical synthesis approach, however, provides the opportunity to obtain a novel insight into such a system and to observe the reactions between individual starting materials separately. In the specific case, the $AlCl_3$ mediated coupling of the monomer TPB and of the nitrogen-containing node CyCl without the addition of DCM neither resulted in the formation of an insoluble (**CTN-7**; see Table S1, Supporting Information), nor of a soluble polymer (Figure S8, Supporting Information). Furthermore, the addition of non-halogenated liquid-assisted grinding agents, such as methanol, ethanol, isopropanol, or ethyl acetate, did not achieve the polymer formation either (see Table S1, Supporting Information). Since only the addition of DCM was capable to accomplish the formation of a highly porous polymer with a theoretically ideal C/N ratio, it has to be classified as a linker rather than as a liquid-assisted grinding agent in the mechanochemical polymerization.

Evidence for this is provided by solid-state nuclear magnetic resonance (NMR) spectroscopy. Figure 3I presents the $^1H \rightarrow {}^{13}C$ cross-polarization magnetic-angle-spinning (CP MAS) spectrum of **CTN-1**. In Figure 3II a tentative assignment of the signals to structure moieties in the polymer is given. In the $^1H \rightarrow {}^{13}C$ CP MAS spectrum (Figure 3I) two broad signals at 140.5 and 128.5 ppm with their corresponding spinning side bands are visible, which can be assigned to the quaternary carbons (A,C,F) and the hydrogen-bonded carbons (B,D,E) of the aromatic units, respectively (Figure 3II). First indication of the incorporation of DCM in the polymer is provided by the broad signal at 37 ppm, which is attributed to a CH_2 (I) group bridging two aromatic moieties. This can occur between two triphenylbenzene moieties or between a triphenylbenzene and a triazine moiety, respectively, which are not distinguishable via the chemical shift in the solid-state NMR spectrum. Additionally, this incorporation of DCM is backed by a $^1H \rightarrow {}^{13}C$ Frequency Switched Lee-Goldburg Heteronuclear Correlation/total

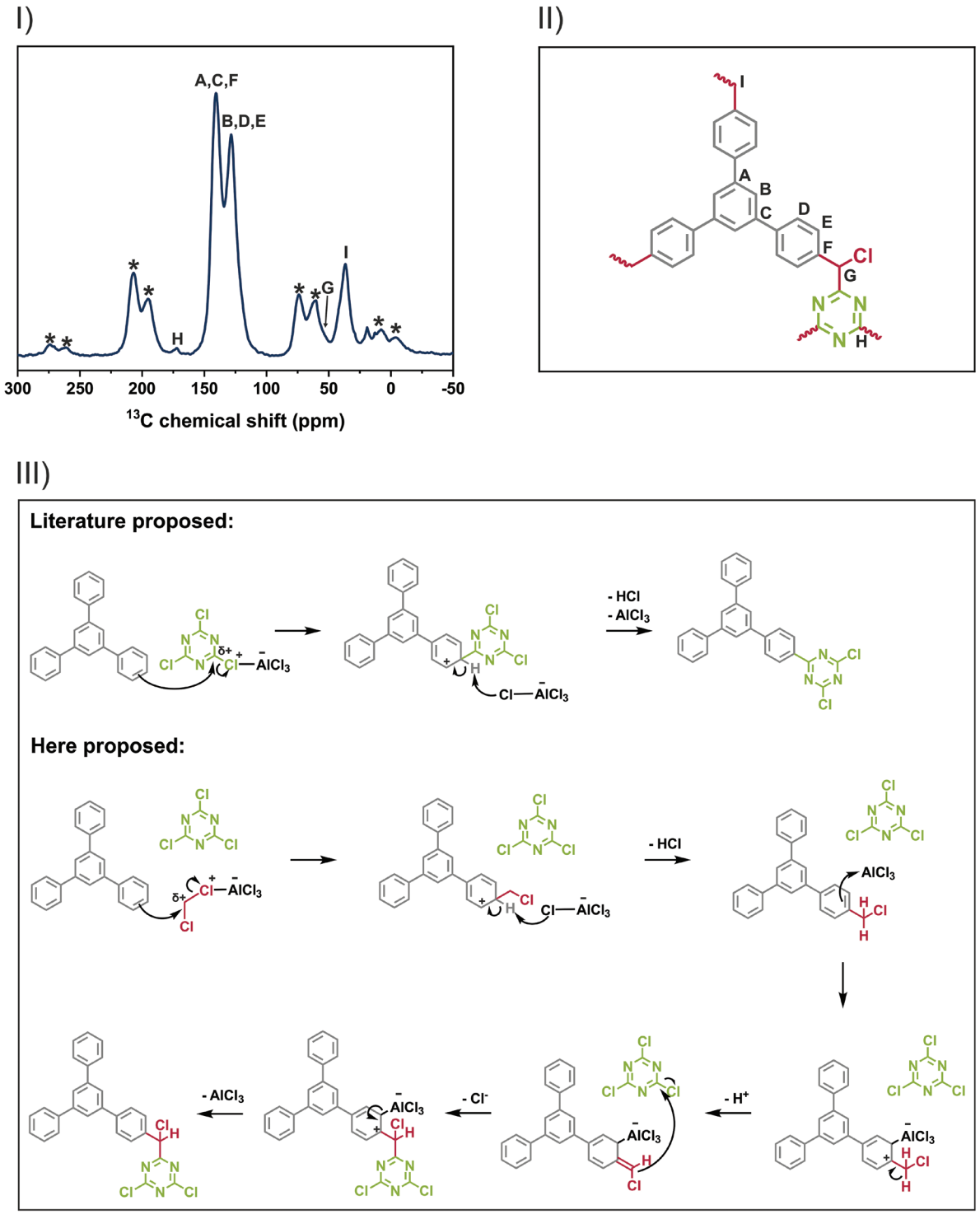

Figure 3. I) $^{1}H \rightarrow {}^{13}C$ CP MAS spectrum of **CTN-1** recorded at 10 kHz spinning. The peaks are labeled as (A-I) and spinning sidebands are assigned with an asterisk. As signal G is masked by a spinning side band, a $^{1}H \rightarrow {}^{13}C$ CP MAS spectrum of **CTN-1** recorded at 8 kHz spinning is depicted in the SI. II) Proposed structure of **CTN-1** and assignment of the labels A-I from the $^{1}H \rightarrow {}^{13}C$ CP MAS spectrum. III) Top: Reaction mechanism of TPB, CyCl, and $AlCl_3$ as proposed in literature. $AlCl_3$ is attacked by one of the chlorine atoms of cyanuric chloride, leading to a positive charge at the carbon atom of the node. This carbon is attacked by the high electron density of TPB, followed by rearomatization of the monomer under the release of HCl. Bottom: Reaction mechanism of TPB, CyCl, DCM, and $AlCl_3$ as proposed here. $AlCl_3$ is attacked by the chlorine of the aliphatic linker, leading to a positive charge at the carbon atom. This carbon is attacked by the high electron density of TPB. The rearomatization occurs due to the attack of $AlCl_4^-$ under the release of HCl. In a next step $AlCl_3$ is attacked by the high electron density of the aromatic ring, resulting in a carbenium ion and in the formation of a double bond under the abstraction of H^+, which allows the nucleophilic attack at the cyanuric chloride. The release of Cl^- from the node $AlCl_3$ leads to rearomatization of the TPB, creating the final product linked over a C1 bridge.

sideband suppression (FSLG HETCOR TOSS) spectrum of **CTN-1**, clearly showing the close proximity between aliphatic and aromatic moieties in the polymer (see Figure S9, Supporting Information). Next, a signal at 60.5 ppm is visible which is masked by spinning sidebands in the 10 kHz spectrum as confirmed by comparison with the spectrum obtained at 8 kHz (see Figure S10, Supporting Information). This signal is assigned to CHCl moieties (G). Finally, a tiny signal at 173 ppm is visible which is attributed to carbons in the triazine rings (H), for which the polarization transfer in $^{1}H \rightarrow {}^{13}C$ CP MAS NMR is less efficient, since they do not contain protons in close proximity. The structure presented in Figure 3II is in line with a possible synthesis mechanism, circumventing the attack of the $AlCl_3$ at the node:

$AlCl_3$ is preferentially attacked by halogen atoms bonded to aliphatic carbons, such as it is the case for DCM (Figure 3III, Bottom). The abstraction of the chlorine by $AlCl_3$ leads to a positive charge on the carbon, capable of being attacked by the nucleophilic monomer, followed by the release of HCl and rearomatization. Next, the high electron density of the ring can attack another $AlCl_3$ molecule, which leads to the formation of a double bond at the C1 moiety under the release of H^+ and is capable to attack the CyCl in a nucleophilic manner. The release of Cl^- and $AlCl_3$ leads to rearomatization and the formation of the final product, linked over the C1 bridge.

To examine the proposed reaction mechanism further, ^{13}C-NMR measurements (200 MHz, Acetone-d_6) were conducted for CTN syntheses at shorter reaction times to capture the formation of smaller oligomers. However, even for a reaction time of only 1 min (see Table S1, Supporting Information, **CTN-1** min) solely a small amount of starting material was dissolving in the deuterated solvent, as the polymer formation was already nearly completed with a yield of 88%. This observation is very interesting, as the introduction of CyCl to the reaction mixture is enhancing the reaction speed by far (**FC-DCM-1**: yield of 41% after 5 min).[39] In addition to this, the SSA_{BET} of **CTN-1** min was already found to be relatively high with 989 $m^2\ g^{-1}$, while the polymer was featuring a C/N ratio of 15.40, allowing the operator to stop the synthesis even after 1 min to exhibit a highly porous and nitrogen-rich polymer. Due to this, the mechanochemical procedure was found to be a highly efficient synthesis tool to circumvent the unfavorable synthesis times of 16 h or more in solution.[27,35,36] Furthermore, the solvent-free approach results in a drastic reduction of hazardous waste, lowering the E-factor from 50.18 (solution-based CTN synthesis) to 9.33 (mechanochemical CTN synthesis) (see Equation (S1), Supporting Information). In order to facilitate an even more ecological synthesis, the amount of $AlCl_3$ utilized in this reaction could be reduced to 12 equiv. to maintain an adequate filling degree of the milling jar, while generating a nitrogen-rich polymer with a yield of 99% and a SSA_{BET} of 1216 $m^2\ g^{-1}$ (see Table S1, Supporting Information).

To prove the linkage over the carbon bridge, employing a monomer already possessing the C1 moiety, such as 4,4′-bis(chloromethyl)1,1′-biphenyl (BCMBP), should lead to a reaction with CyCl even without the addition of DCM. Indeed, the respective polymer **CTN-BCMBP** was obtained in 77% yield and with a C/N ratio of 8.80 (see Table S1 and Figure S11I, Supporting Information). To confirm this observation, the same reaction was carried out with biphenyl as monomer (without C1 moiety), not leading to the generation of any product (Figure S11II). As a third verification step, the biphenyl reaction was performed with the addition of DCM, which again resulted in the formation of a nitrogen-containing porous polymer (**CTN-BP-2**, Figure S11III, Supporting Information). To verify the formation of a C1 bridge in the model compounds, $^{1}H \rightarrow {}^{13}C$ CP MAS spectra were recorded for **CTN-BCMBP** (Figure S12, Supporting Information) and for **CTN-BP-2** (Figure S13, Supporting Information), both featuring the signals I and K attributed to the formation of CHCl and CH_2 moieties, respectively. Furthermore, both spectra feature a high resemblance, indicating the formation of two similar polymers by different synthetic approaches.

Applying this concept further, two possibilities arise for the post polymerization (PPM) functionalization of already synthesized polymers. In case of a carbon and hydrogen-containing polymer without C1 moiety (**PP1**), the milling with $AlCl_3$, CyCl, and DCM leads to the formation of a nitrogen-containing polymer with a SSA_{BET} of 1258 $m^2\ g^{-1}$, nearly doubling the specific surface area of the original polymer (see Table S1, Supporting Information, **CTN-PPM-1**).[42] In the case of a carbon and hydrogen-containing polymer featuring a C1 moiety (**FC-DCM-1**), it is furthermore possible to introduce nitrogen into the polymer without the addition of DCM during the post polymerization (see Table S1, Supporting Information, **CTN-PPM-2**).

Through these experiments, it was confirmed that the C1 moiety, serving as a linkage point, is crucial for the reaction with CyCl. Thereby, the DCM does not need to be present in the reaction mixture, precluding its role as a liquid-assisted grinding agent or as a solvent, as long as the C1 moiety is already present in the monomer or in the polymer being functionalized.

2.3. Variation of Linker, Node, and Monomer

In order to examine the special role of the linker as a C1 bridge further, the equivalent amount of DCM was varied, while keeping the quantity of co-reactants constant (1 equiv. TPB and 6 equiv. CyCl). In addition to the dependency on the amount of node utilized, the specific surface areas of CTNs are highly dependent on the amount of linker added to the reaction mixture. Thereby it was possible to vary the SSA_{BET} between 46 $m^2\ g^{-1}$ for the addition of 1 equiv. DCM (**CTN-DCM-1**) and 1136 $m^2\ g^{-1}$ for the addition of 6 equiv. of DCM (**CTN-1**) (see **Figure 4**I). However, the use of lower amounts of linker did not affect the linkage with CyCl over the introduced C1 moiety. Even for the polymerization with only 1 equiv. of linker, the C/N ratio of the polymer **CTN-DCM-1** was found to be theoretically ideal for the incorporation of 1 equiv. of node (measured value: 9.73; theoretical value: 9.33).

Due to these results, the utilization of other halogenated liquids as linkers was found to be particularly interesting to achieve a variation of the pore geometry and polymer flexibility.[39] Therefore, DCM was substituted by $CHCl_3$, which was added to the reaction mixture in various equimolar amounts (see Figure S14, Supporting Information). In comparison to the DCM linkage, the specific surface areas of the respective CTNs were much higher, as $CHCl_3$ is capable to form highly rigid

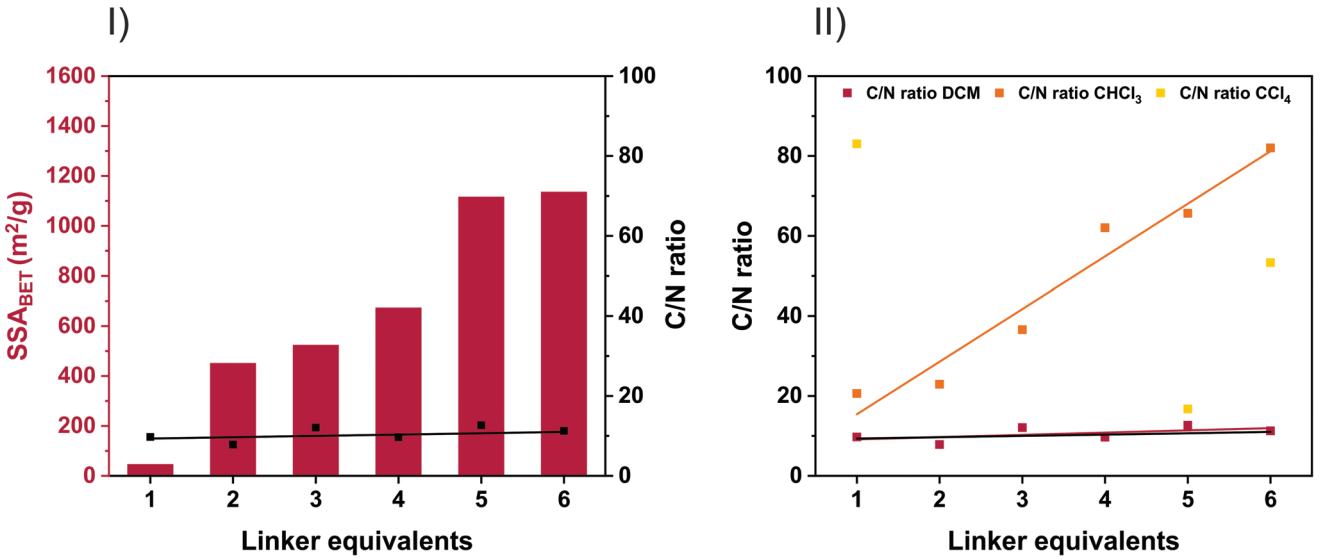

Figure 4. I) Variation of DCM equivalent for a polymerization with 6 equiv. CyCl and 1 equiv. TPB and the dependency of SSA_{BET} (red bars) and C/N ratio (black squares) of the respective CTNs. The solid black line indicates the theoretical C/N ratio for each sample and fits the measured values. II) C/N ratios for the variation of linker equivalents of DCM (red squares), $CHCl_3$ (orange squares), and CCl_4 (yellow squares) for a polymerization with 6 equiv. CyCl and 1 equiv. TPB. Solid orange line: linear fit of orange squares; Solid red line: linear fit of red squares; Solid black line: theoretical C/N ratios. For the addition of 2–4 equiv. of CCl_4 no nitrogen was found in the respective polymers.

polymers, exhibiting a well-defined pore structure (Figure S14, Supporting Information). However, the amount of node incorporated into the polymer was found to be considerably smaller than for the linkage with DCM. This has two reasons: The addition of more equivalents of $CHCl_3$ leads to a higher rigidity of the polymer, which hinders the incorporation of CyCl. This is visible in Figure 4II, as a higher amount of $CHCl_3$ equivalents leads to higher C/N ratios (orange squares). Furthermore, the abstraction of the hydrogen from the $CHCl_2$ bridge, formed by the reaction of the monomer and the $CHCl_3$, is more difficult than from the CH_2Cl moiety, formed with DCM as linker.

In order to proof this, CCl_4 was utilized as a linker, as the lack of hydrogen bonded to the C1 moiety should lead to no reaction with the CyCl and therefore to no nitrogen present in the polymer. Although for the utilization of 1 equiv. of CCl_4 a very small amount of nitrogen was found in the polymer **CTN-CCl_4-1** (C/N ratio: 83.03 = 1.08 at%), which might be due to an incomplete washing procedure, the addition of 2–4 equiv. indeed did not lead to any incorporation of nitrogen (see yellow squares in Figure 4II and Table S1, Supporting Information). For an addition of 5 and 6 equiv. of CCl_4, CyCl was again present in the final product, however not as a part of the polymer itself. As both reactions resulted in a yield of 197% and 236%, respectively, as well as in specific surface areas of <1 $m^2\ g^{-1}$, the high amount of linking agent was found to lead to a very rigid polymer, trapping the node inside the pores (Figure S15, Supporting Information).

Although the variation of the linker underlined the proposed reaction mechanism over the C1 bridge by abstraction of hydrogen from the same, it was not very promising for the generation of nitrogen-containing polymers with various pore geometries. However, another possibility to achieve this is by the replacement of the node. Instead of CyCl, linear or angled nitrogen-containing nodes could be considered. Therefore, the linear 3,6-dichloropyridazine (DCD) was compared with the angled 4,6-dichloropyrimidine (DCY) and 2,6-dichloropyrazine (DCP) as CyCl substitution (see **Figure 5**I). For the synthesis of **CTN-DCD** with DCD utilized as node, only a small amount was incorporated into the polymer, which can be seen by high C/N ratio of 75.23. One reason for this could be the para position of the two chlorine-bonded carbon atoms. However, since the utilization of nodes with the two chlorine-bonded carbons in meta-position gave very different results (see Figure 5I), it was found that the position of the nitrogens relative to each other was most important for the incorporation of the node into the polymer. While DCY (meta position of Ns) was incorporated very well into the polymer (**CTN-DCY** C/N ratio: 11.60), the substitution with DCP (para position of Ns) resulted in lower amounts of the node being integrated in the polymer (**CTN-DCP** C/N ratio: 40.71) (see Figure 5I and Table S1, Supporting Information). Nevertheless, DCP serves as the best porogen, capable of achieving an SSA_{BET} of 1518 $m^2\ g^{-1}$ of the final polymer.

Besides the linker and the node, the monomer can be replaced as well. Regardless of the monomer utilized for the replacement, all polymers obtained were exhibiting high specific surface areas and yields, accompanied by almost ideal C/N ratios (see Figure 5II and Table S1, Supporting Information). Therefore, the monomer replacement proved to be the most promising method to modify the structural properties of CTNs. Due to the parameter setting, it was even possible to achieve the formation of a porous and nitrogen-containing polymer with benzene as monomer (see Figure 5II), which was rather difficult in the past.[48] Moreover, the utilization of triptycene enabled the formation of a highly porous CTN, exhibiting an SSA_{BET} of 1502 $m^2\ g^{-1}$ with a C/N ratio of 13.62.

Thus, by varying the different building blocks of the mechanochemical reaction, a wide variety of nitrogen-containing

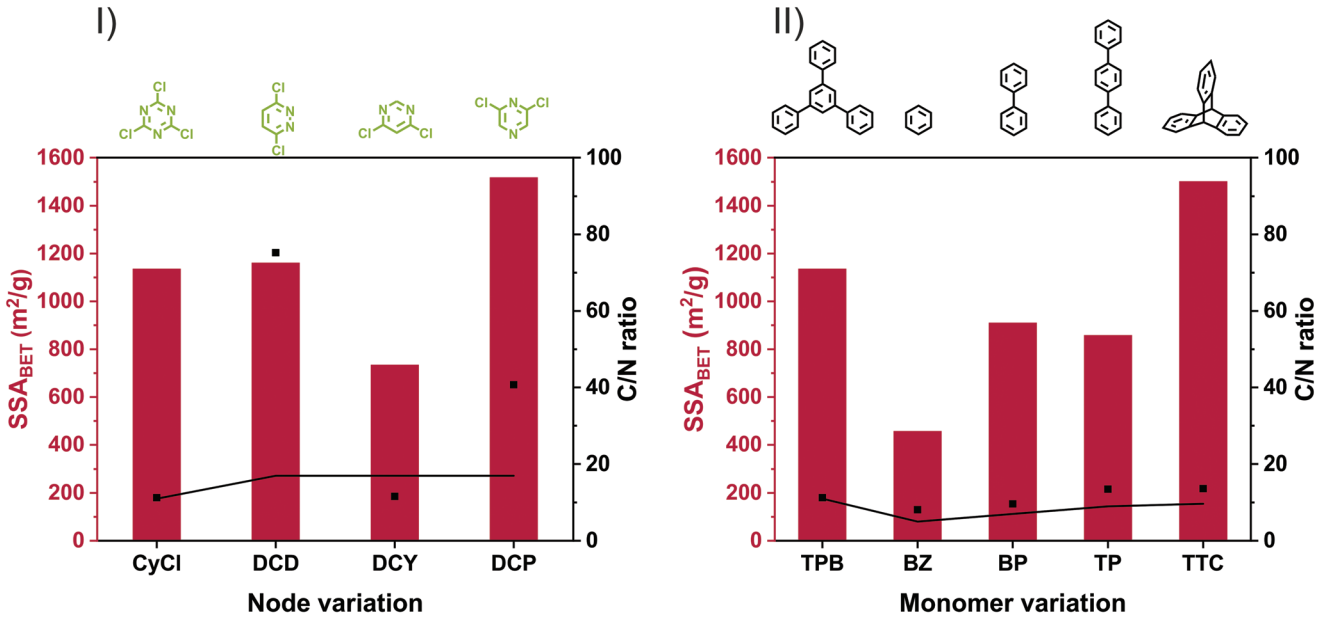

Figure 5. I) Variation of the node (each 6 equiv.) for a polymerization with 6 equiv. DCM and 1 equiv. TPB and the dependency of SSA_{BET} (red bars) and C/N ratio (black squares) of the respective CTNs. The solid black line indicates the theoretical C/N ratios. II) Variation of the Monomer (each 1 equiv.) for a polymerization with 6 equiv. DCM and 6 equiv. CyCl and the dependency of SSA_{BET} (red bars) and C/N ratio (black squares) of the respective CTNs. The solid black line indicates the theoretical C/N ratios.

polymers can be produced and can be tailored to the desired properties by a simple, rapid, and sustainable synthesis.

3. Conclusion

Herein we presented the sustainable generation of various CTNs by a simple and rapid mechanochemical synthesis approach, which even enabled the formation of a highly porous and nitrogen-containing polymer after only 1 min of reaction time. By this approach, it was possible to identify the special role of the node, acting as a porogen for pore formation in this reaction. Additionally, although formerly considered to act only as a solvent, the solvent-free synthesis approach enabled to identify DCM as a crucial linker, capable to knit the nitrogen-containing node and the aromatic monomer over a C1 bridge. This observation even resulted in the successful post polymerization functionalization of already synthesized carbon and hydrogen-containing polymers. Moreover, the variation of linker, node, and monomer prompted the synthesis of polymers with specific surface areas of more than 1500 $m^2\ g^{-1}$, exhibiting an almost ideal C/N ratio. The presented approach was therefore considered to be highly suitable for the sustainable synthesis of CTNs.

4. Experimental Section

Mechanochemical CTN Synthesis: In a typical synthesis approach, 0.50 g (1.63 mmol, 1 equiv.) TPB, 1.81 g (9.79 mmol, 6 equiv.) CyCl, and 0.63 mL (9.79 mmol, 6 equiv.) DCM were brought to reaction by utilizing $AlCl_3$ (5.22 g, 39.16 mmol, 24 equiv.) simultaneously as Lewis acid and as bulking material. The reaction was accomplished by milling the starting materials under inert gas atmosphere in a 50 mL ZrO_2 milling jar, equipped with 22 ZrO_2 milling balls (ø = 10 mm, average weight 3.2 g), for 1 h at 30 Hz in a Retsch MM500 mixer mill. Subsequent to the milling, the reaction mixture was washed with water and acetone, yielding a brown polymer, which was dried at 80 °C overnight.

Analysis: Physisorption measurements were carried out with high purity nitrogen gas (N_2: 99.99%) on a Quantachrome Quadrasorb instrument at 77 K. All samples were outgassed for 24 h at 423 K prior to the measurement. To determine the specific surface areas (SSA) the BET (Brunauer, Emmett, Teller) equation was utilized. Total pore volumes were estimated at the adsorption branch at $P/P_0 = 0.95$ and pore size distributions were calculated utilizing the DFT (density functional theory) method for slit pores. As the nitrogen-containing polymers were more hydrophilic than a purely carbon-containing polymer, the utilization of a carbon-based calculation model resulted in a slight overestimation of the specific surface area and of a slight underestimation of the pore size. However, the model was found to be most sufficient for the calculation and is presenting a good approximation to the real conditions. In addition, H_2O adsorption measurements were performed on a Quantachrome Autosorb instrument at 298 K. Prior to the measurement, the samples were outgassed in a similar fashion to aforementioned.

Infrared spectroscopy spectra were recorded with 16 scans between 500 and 3500 cm^{-1} using a SHIMADZU IRSpirit Fourier transform infrared spectrometer equipped with a diffuse reflectance device.

XPS measurements were performed on a Nexsa G2 Surface Analysis System with a monochromatic Al Kα X-ray source utilizing a 128-channel detector.

SEM images were recorded with the JEOL JSM-IT800SHL instrument at a voltage of 15 kV.

All solid-state NMR spectra were recorded on a Bruker Avance III 600 MHz spectrometer at 14.1 T corresponding to frequencies of 600.11 and 150.91 MHz for ^1H and ^{13}C, respectively. The spectra were acquired with a 4 mm $^1H/X$ double resonance probe.

$^1H \rightarrow {}^{13}C$ CP MAS spectra were recorded at 8 and 10 kHz spinning. The contact time was set to 2.5 ms and a linear 100–50 ramp was applied on the ^1H channel during contact. The recycle delay was set to 1 s and the acquisition time to 20 ms and a Two pulse phase modulation (TPPM) decoupling sequence was applied during data acquisition. Spectra were recorded with 4096 scans and referenced to TMS (0 ppm) with adamantane (38.5 ppm) as an external standard.

The $^{1}H \rightarrow {}^{13}C$ FSLG HETCOR TOSS spectrum was recorded at 8 kHz spinning. A $\pi/2$ excitation pulse of 2.5 µs was applied on the ^{1}H channel. During evolution of the chemical shift, frequency switched Lee-Goldburg (FSLG) homonuclear decoupling with a 80 kHz field was applied.[56] The contact time was set to 0.5 ms and a linear 100–50 ramp was applied on the ^{1}H channel during contact. To suppress spinning side bands the total suppression of spinning sidebands (TOSS) sequence was applied on the ^{13}C channel employing π pulses of 9.4 µs.[57] The recycle delay was set to 1 s. TPPM heteronuclear decoupling was performed during data acquisition.[58] The spectrum was measured with 64 slices each with 2560 scans. The ^{13}C dimension was referenced to TMS (0 ppm) with adamantane (38.5 ppm) as an external standard. The ^{1}H dimension was referenced to TMS employing the procedure described in the literature.[59]

Supporting Information

Supporting Information is available from the Wiley Online Library or from the author.

Acknowledgements

The authors gratefully acknowledge the Federal Ministry of Education and Research (Bundesministerium für Bildung und Forschung, BMBF) for support of the Mechanocarb project (award number 03SF0498). T.G. and M.V.H. thank the DFG under contract GU-1650/3-1 for financial support. The authors thank Prof. Buntkowsky for generous allocation of measurement-time at his 600 MHz spectrometer in Darmstadt.

Open access funding enabled and organized by Projekt DEAL.

Conflict of Interest

The authors declare no conflict of interest.

Data Availability Statement

The data that support the findings of this study are available from the corresponding author upon reasonable request.

Keywords

ball milling, covalent triazine networks, mechanochemistry, microporous polymers, solvent-free synthesis, sustainable synthesis

Received: November 17, 2022
Revised: December 20, 2022
Published online: February 9, 2023

[1] S. Kim, B. Kim, N. A. Dogan, C. T. Yavuz, *ACS Sustainable Chem. Eng.* **2019**, *7*, 10865.
[2] Q. Sun, Z. Dai, X. Meng, F.-S. Xiao, *Chem. Soc. Rev.* **2015**, *44*, 6018.
[3] K. Dong, Q. Sun, X. Meng, F.-S. Xiao, *Catal. Sci. Technol.* **2017**, *7*, 1028.
[4] N. B. McKeown, P. M. Budd, *Chem. Soc. Rev.* **2006**, *35*, 675.
[5] C. Özen, K. Obata, P. Bogdanoff, N. Yulianto, H. S. Wasisto, F. F. Abdi, *Sustainable Energy Fuels* **2022**, *6*, 377.
[6] A. Li, R.-F. Lu, Y. Wang, X. Wang, K.-L. Han, W.-Q. Deng, *Angew. Chem., Int. Ed.* **2010**, *49*, 3330.
[7] V. Rozyyev, D. Thirion, R. Ullah, J. Lee, M. Jung, H. Oh, M. Atilhan, C. T. Yavuz, *Nat. Energy* **2019**, *4*, 604.
[8] W. Lu, D. Yuan, D. Zhao, C. I. Schilling, O. Plietzsch, T. Muller, S. Bräse, J. Guenther, J. Blümel, R. Krishna, Z. Li, H.-C. Zhou, *Chem. Mater.* **2010**, *22*, 5964.
[9] Q. Pujol, G. Weber, J.-P. Bellat, S. Grätz, A. Krusenbaum, L. Borchardt, I. Bezverkhyy, *Microporous Mesoporous Mater.* **2022**, *344*, 112204.
[10] B. Zhang, W. Wang, L. Liang, Z. Xu, X. Li, S. Qiao, *Coord. Chem. Rev.* **2021**, *436*, 213782.
[11] S. Chuhadiya, Himanshu, D. Suthar, S. L. Patel, M. S. Dhaka, *Coord. Chem. Rev.* **2021**, *446*, 214115.
[12] K. Amin, N. Ashraf, L. Mao, C. F. Faul, Z. Wei, *Nano Energy* **2021**, *85*, 105958.
[13] D.-H. Yang, Y. Tao, X. Ding, B.-H. Han, *Chem. Soc. Rev.* **2022**, *51*, 761.
[14] K. Cousins, R. Zhang, *Polymers* **2019**, *11*, 690.
[15] P. Kaur, J. T. Hupp, S. T. Nguyen, *ACS Catal.* **2011**, *1*, 819.
[16] P. Kuhn, A. Thomas, M. Antonietti, *Macromolecules* **2009**, *42*, 319.
[17] P. Kuhn, K. Krüger, A. Thomas, M. Antonietti, *Chem. Commun.* **2008**, *2008*, 5815.
[18] H. Chen, X. Suo, Z. Yang, S. Dai, *Adv. Mater.* **2022**, *34*, 2107947.
[19] Y. Li, C. Lai, S. Liu, Y. Fu, L. Qin, M. Xu, D. Ma, X. Zhou, F. Xu, H. Liu, L. Li, Q. Sun, N. Wang, *J. Mater. Chem. A* **2023**.
[20] A. Thomas, *Angew. Chem., Int. Ed.* **2010**, *49*, 8328.
[21] R. Palkovits, M. Antonietti, P. Kuhn, A. Thomas, F. Schüth, *Angew. Chem., Int. Ed.* **2009**, *48*, 6909.
[22] P. Puthiaraj, W.-S. Ahn, *Catal. Sci. Technol.* **2016**, *6*, 1701.
[23] C. E. Chan-Thaw, A. Villa, P. Katekomol, D. Su, A. Thomas, L. Prati, *Nano Lett.* **2010**, *10*, 537.
[24] S. Ren, M. J. Bojdys, R. Dawson, A. Laybourn, Y. Z. Khimyak, D. J. Adams, A. I. Cooper, *Adv. Mater.* **2012**, *24*, 2357.
[25] A. Bhunia, V. Vasylyeva, C. Janiak, *Chem. Commun.* **2013**, *49*, 3961.
[26] A. Bhunia, D. Esquivel, S. Dey, R. Fernández-Terán, Y. Goto, S. Inagaki, P. van der Voort, C. Janiak, *J. Mater. Chem. A* **2016**, *4*, 13450.
[27] Z. Jia, J. Pan, D. Yuan, *ChemistryOpen* **2017**, *6*, 554.
[28] N. Taheri, M. Dinari, M. Asgari, *ACS Appl Polym Mater* **2022**, *4*, 6288.
[29] L. Meng, X. Zou, S. Guo, H. Ma, Y. Zhao, G. Zhu, *ACS Appl. Mater. Interfaces* **2015**, *7*, 15561.
[30] P. Kuhn, M. Antonietti, A. Thomas, *Angew. Chem., Int. Ed.* **2008**, *47*, 3450.
[31] P. Kuhn, A. Forget, J. Hartmann, A. Thomas, M. Antonietti, *Adv. Mater.* **2009**, *21*, 897.
[32] M. G. Mohamed, A. F. M. El-Mahdy, Y. Takashi, S.-W. Kuo, *New J. Chem.* **2020**, *44*, 8241.
[33] Z.-A. Lan, M. Wu, Z. Fang, Y. Zhang, X. Chen, G. Zhang, X. Wang, *Angew. Chem., Int. Ed.* **2022**, *61*, e202201482.
[34] W. Zhang, C. Li, Y.-P. Yuan, L.-G. Qiu, A.-J. Xie, Y.-H. Shen, J.-F. Zhu, *J. Mater. Chem.* **2010**, *20*, 6413.
[35] S. Dey, A. Bhunia, D. Esquivel, C. Janiak, *J. Mater. Chem. A* **2016**, *4*, 6259.
[36] H. Lim, M. C. Cha, J. Y. Chang, *Macromol. Chem. Phys.* **2012**, *213*, 1385.
[37] P. Puthiaraj, S.-M. Cho, Y.-R. Lee, W.-S. Ahn, *J. Mater. Chem. A* **2015**, *3*, 6792.
[38] A. Krusenbaum, S. Grätz, G. T. Tigineh, L. Borchardt, J. G. Kim, *Chem. Soc. Rev.* **2022**, *51*, 2873.
[39] A. Krusenbaum, J. Geisler, F. J. L. Kraus, S. Grätz, M. V. Höfler, T. Gutmann, L. Borchardt, *J. Polym. Sci.* **2022**, *60*, 62.
[40] S. Grätz, M. Oltermann, E. Troschke, S. Paasch, S. Krause, E. Brunner, L. Borchardt, *J. Mater. Chem. A* **2018**, *6*, 21901.
[41] R. Yuan, Z. Yan, A. Shaga, H. He, *J. Solid State Chem.* **2020**, *287*, 121327.
[42] A. Krusenbaum, S. Grätz, S. Bimmermann, S. Hutsch, L. Borchardt, *RSC Adv.* **2020**, *10*, 25509.
[43] S. Grätz, S. Zink, H. Kraffczyk, M. Rose, L. Borchardt, *Beilstein J. Org. Chem.* **2019**, *15*, 1154.

[44] J.-S. M. Lee, T. Kurihara, S. Horike, *Chem. Mater.* **2020**, *32*, 7694.
[45] Q. Pan, Z. Xu, S. Deng, F. Zhang, H. Li, Y. Cheng, L. Wei, J. Wang, B. Zhou, *RSC Adv.* **2019**, *9*, 39332.
[46] X. Zhu, C. Tian, T. Jin, K. L. Browning, R. L. Sacci, G. M. Veith, S. Dai, *ACS Macro Lett.* **2017**, *6*, 1056.
[47] X. Zhu, Y. Hua, C. Tian, C. W. Abney, P. Zhang, T. Jin, G. Liu, K. L. Browning, R. L. Sacci, G. M. Veith, H.-C. Zhou, W. Jin, S. Dai, *Angew. Chem., Int. Ed.* **2018**, *57*, 2816.
[48] E. Troschke, S. Grätz, T. Lübken, L. Borchardt, *Angew. Chem., Int. Ed.* **2017**, *56*, 6859.
[49] P. Puthiaraj, S.-S. Kim, W.-S. Ahn, *Chem. Eng. J.* **2016**, *283*, 184.
[50] A. Rengaraj, P. Puthiaraj, Y. Haldorai, N. S. Heo, S.-K. Hwang, Y.-K. Han, S. Kwon, W.-S. Ahn, Y. S. Huh, *ACS Appl. Mater. Interfaces* **2016**, *8*, 8947.
[51] W. Zhao, H. Zuo, Y. Guo, K. Liu, S. Wang, L. He, X. Jiang, G. Xiang, S. Zhang, *Talanta* **2019**, *201*, 426.
[52] Y. Shi, K. Hu, Y. Cui, J. Cheng, W. Zhao, X. Li, *Microchem. J.* **2019**, *146*, 525.
[53] V. Rozyyev, Y. Hong, M. S. Yavuz, D. Thirion, C. T. Yavuz, *Adv. Energy Sustainability Res.* **2021**, *2*, 2100064.
[54] S. Wang, C. Zhang, Y. Shu, S. Jiang, Q. Xia, L. Chen, S. Jin, I. Hussain, A. I. Cooper, B. Tan, *Sci. Adv.* **2017**, *3*, e1602610.
[55] K. P. C. Vollhardt, N. E. Schore, *Organic Chemistry; Structure and Functions*, 5th ed., W.H. Freeman, New York **2007**.
[56] B.-J. van Rossum, H. Förster, H. de Groot, *J. Magn. Reson.* **1997**, *124*, 516.
[57] W. Dixon, J. Schaefer, M. Sefcik, E. Stejskal, R. McKay, *J. Magn. Reson.* **1982**, *49*, 341.
[58] A. E. Bennett, C. M. Rienstra, M. Auger, K. V. Lakshmi, R. G. Griffin, *J. Chem. Phys.* **1995**, *103*, 6951.
[59] B. Kumari, M. Brodrecht, T. Gutmann, H. Breitzke, G. Buntkowsky, *Appl. Magn. Reson.* **2019**, *50*, 1399.